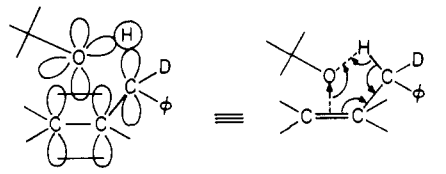

Figure 1.

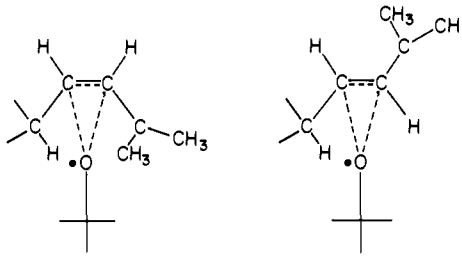

Figure 2.

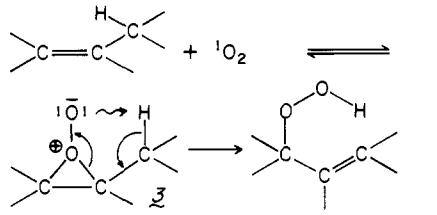

Figure 3.

the bulky *tert*-butoxy radical more than twice as fast as the hindered cis. They attributed the rate difference to the relative stabilities of the cis (**2a**) and trans (**2b**) π complexes shown in Figure 2. (The dotted lines in Figure 2 represent a complexing interaction between the oxygen and the olefinic centers.)

The analogous deduction can be made regarding the geometry of the allylic H-transfer transition state in the electrophilic mechanism of hydroperoxidation of olefins by singlet oxygen.[13] By most criteria which have been previously applied,[14] including the magnitude of k_H/k_D at a single temperature,[14e] it has not been possible to distinguish unequivocally between a concerted ene-reaction transition state and a cheletropic mechanism involving formation of a transient perepoxide intermediate. However, Bartlett and co-workers[15] have provided elegant justification of the perepoxide intermediate through a laboriously detailed study of kinetic and product isotope effects in singlet oxygen hydroperoxidation of 4-methyl-2,3-dihydro-γ-pyran. This conclusion, implying a bent transition state of H transfer taking place subsequent to the formation of σ perepoxide complex **3**, is fully supported by the data assembled in Table II. They confirm a temperature-independent isotope effect greater than the maximum theoretical value of A_H/A_D in keeping with the mechanistic course illustrated in Figure 3.

Finally, it is of considerable interest to take note of the nature of the kinetic isotope effect in the homolytic abstraction of benzylic hydrogen by *tert*-butoxy radical,[17] where the hydrogen donor substrate, toluene, does not possess the ability to tightly complex the *tert*-butoxy radical acceptor. Larson and Gilliom[18] have studied the case of toluene in reaction with *tert*-butyl hypochlorite under conditions eliminating chlorine atom chains. The steep temperature dependence of k_H/k_D which they report is taken to be fully consistent with *linear* H transfer involving tunneling, in contrast to the bent transition state (Figure 1) discussed here for allylic olefin centers. The lesser ability of the aromatic nucleus to complex the *tert*-butoxy radical is evident in the fact that the reactant **1**, containing both aromatic and allylic olefin substituents at the site of H abstraction, prefers the bent transition-state pathway conferred by the olefin center.

Table II.[a] Temperature Dependence of the Primary Deuterium Isotope Effect in the Hydroperoxidation of $(CH_3)_2C{=}C(CD_3)_2$ by $^1O_2$

reaction temp, °C,	k_H/k_D[b]
14	1.36
0	1.47
−28	1.45
−52	1.36
−70	1.62
ΔT = 84	k_H/k_D = 1.45 ± 0.07

[a] Data of Kopecky and Van de Sande.[16] [b] Each value listed is the average of a number of determinations with a precision of ±8%.

References and Notes

(1) W. A. Pryor and K. G. Kneipp, *J. Am. Chem. Soc.*, **93**, 5584 (1971).
(2) K. B. Wiberg and E. L. Motell, *Tetrahedron*, **19**, 2009 (1963).
(3) This approach to elucidating transition state geometries has been discussed in theoretical reviews: (a) R. P. Bell, *Chem. Soc. Rev.*, **3**, 513 (1974), and (b) R. A. More O'Ferrall, *J. Chem. Soc. B*, 785 (1970), and R. A. More O'Ferrall, and J. Kouba, *ibid.*, 985 (1967), as well as in various applications, i.e., (c) H. Kwart and M. C. Latimore, *J. Am. Chem. Soc.*, **93**, 3770 (1971); (d) H. Kwart and J. H. Nickle, *ibid.*, **95**, 3394 (1973); (e) H. Kwart, S. F. Sarner, and J. Slutsky, *ibid.*, **95**, 5242 (1973); (f) J. W. A. M. Janssen and H. Kwart, *J. Org. Chem.*, **42**, 1530 (1977).
(4) See for a full discussion, G. Sosnovsky and S.-O. Lawesson, *Angew. Chem., Int. Ed. Engl.*, **3**, 269 (1964).
(5) D. B. Denny, D. Z. Denny, and G. Feig, *Tetrahedron Lett.*, **No. 15**, 19 (1959).
(6) See, for examples and discussion, H. Kwart, T. J. George, R. Louw, and W. Ultee, *J. Am. Chem. Soc.*, **100**, 3927 (1978).
(7) W. J. Albery and J. R. Knowles, *J. Am. Chem. Soc.*, **99**, 637 (1977).
(8) M. E. Schneider and M. J. Stern, *J. Am. Chem. Soc.*, **94**, 1517 (1972), for example, have calculated preexponential factors for five model reactions and find that A_H/A_D lies between 0.75 and 1.2. It has also been calculated previously (see R. P. Bell, *Chem. Soc. Rev.*, 513 (1974)) that, when A_H/A_D is > 1.2, tunneling is unimportant. See J.-H. Kim and K. T. Leffek, *Can. J. Chem.*, **52**, 592 (1974), for a fuller discussion of these maxima and minima of A_H/A_D values in linear H-transfer processes.
(9) Clearly, the radical with the lower energy SOMO will be more reactive (more negative ρ value[10]). This is illustrated by the finding[11] that the *t*-BuOO· radical, where the α effect is operating to make an electrophilic radical less reactive, is 10 000 times less reactive in hydrogen abstraction then *t*-BuO·.
(10) See G. A. Russell in "Free Radicals", Vol. 1, J. Kochi, Ed., Wiley, New York, 1973, p 295, and R. W. Henderson, *J. Am. Chem. Soc.*, **97** 213 (1975).
(11) K. U. Ingold, *Pure Appl. Chem.*, **15**, 49 (1967).
(12) C. Walling and A. Zavitsas, *J. Am. Chem. Soc.*, **85**, 2084 (1963).
(13) C. W. Jefford and C. G. Rimbault, *J. Org. Chem.*, **43**, 1908 (1978).
(14) (a) L. A. Paquette, D. C. Liotta, C. C. Liao, T. G. Walles, N. Eickman, J. Clardy, and R. Gleiter, *J. Am. Chem. Soc.*, **98**, 6413 (1976); (b) L. A. Paquette, D. C. Liotta, and A. D. Baker, *Tetrahedron Lett.*, 2681 (1976); (c) R. W. Denny and A. Nickon, *Org. React.*, **20**, 147 (1973); (d) F. A. Litt and A. Nickon, *Adv. Chem. Ser.*, **No. 77**, III (1968); (e) A. Nickon, V. T. Chuang, P. J. L. Daniels, R. W. Denny, J. B. DiGiorgio, J. Tsunetsugu, H. G. Vilhuber, and E. Werstiuk, *J. Am. Chem. Soc.*, **94**, 5517 (1972).
(15) A. A. Frimer, P. D. Bartlett, A. F. Boschung, and J. G. Jewett, *J. Am. Chem. Soc.*, **99**, 7977 (1977).
(16) K. R. Kopecky and J. H. Van de Sande, *Can. J. Chem.*, **50**, 4034 (1972).
(17) C. Walling and B. B. Jacknow, *J. Am. Chem. Soc.*, **82**, 6108 (1960).
(18) G. I. Larson and R. D. Gilliom, *J. Am. Chem. Soc.*, **97**, 3444 (1975).

H. Kwart,* D. A. Benko, M. E. Bromberg
University of Delaware
Newark, Delaware 19711
June 5, 1978

Transient Proton–Proton Overhauser Effects in Horse Ferrocytochrome *c*

Sir:

The nuclear Overhauser effect (NOE) is the fractional change in intensity of one NMR resonance when another resonance is irradiated, and has long been a valuable tool for structural studies of small molecules.[1] More recently theoretical aspects of using NOE's for investigations of biological macromolecules at high frequencies were discussed,[2] and

0002-7863/78/1500-7094$01.00/0

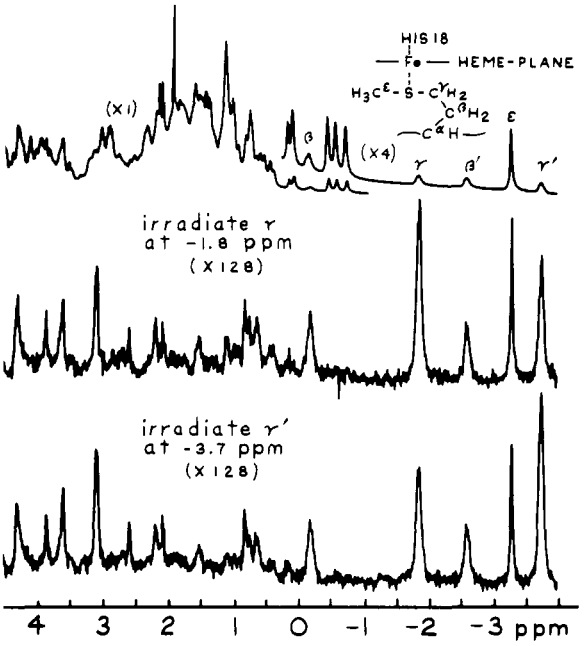

Figure 1. 360-MHz Fourier transform ^{1}H NMR and steady-state NOE difference spectra of a 0.008 M solution of horse heart ferrocytochrome *c* in 0.05 M deuterated phosphate buffer, pD 6.8, $T = 49$ °C. These and the spectra in Figures 2 and 3 were recorded on a Bruker HX-360 spectrometer. The chemical shifts are referenced to internal TSP.[15] The NOE difference spectra were obtained by subtracting spectra with NOE's from reference spectra. The spectra with NOE's were obtained by applying a 2-s low-power saturating pulse at the frequency indicated above each trace, followed immediately by a 90° observation pulse. The reference spectra were obtained by offsetting the saturation pulse to −5 ppm. Each spectrum was the result of 2000 accumulations. The NOE and reference spectrum FID's[16] were accumulated alternately in order to minimize drifts.

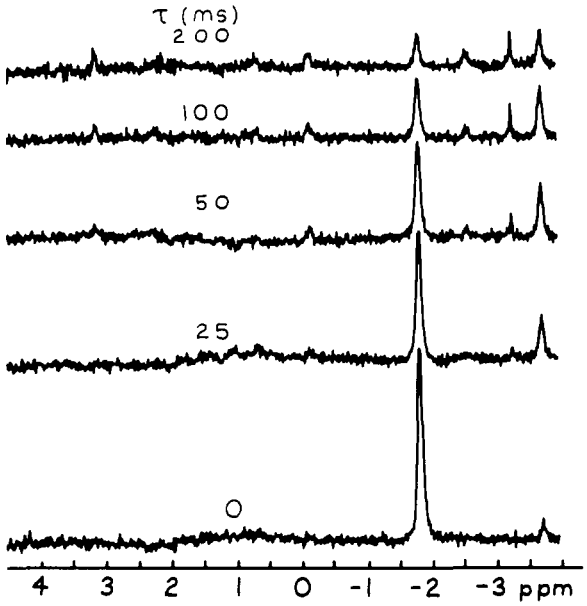

Figure 2. Transient NOE difference spectra resulting from inversion of the Met 80 γ-proton resonance. Values of the delay time τ in milliseconds are given above each spectrum. The difference spectra here and in Figure 3 were obtained by subtracting spectra with transient NOE's from reference spectra. Spectra with transient NOE's were obtained by applying a 15-ms inversion pulse at the γ resonance frequency (−1.8 ppm) followed, after a delay time τ, by a 90° observation pulse. The reference spectra were obtained by offsetting the inversion pulse to −5 ppm. Each spectrum was the result of 1000 accumulations. The NOE and reference spectrum FID's were accumulated alternately in order to minimize instrumental drifts.

several applications of ^{1}H-^{1}H NOE experiments for improving the spectral resolution and assigning individual resonances in the ^{1}H NMR spectra of proteins, as well as for characterization

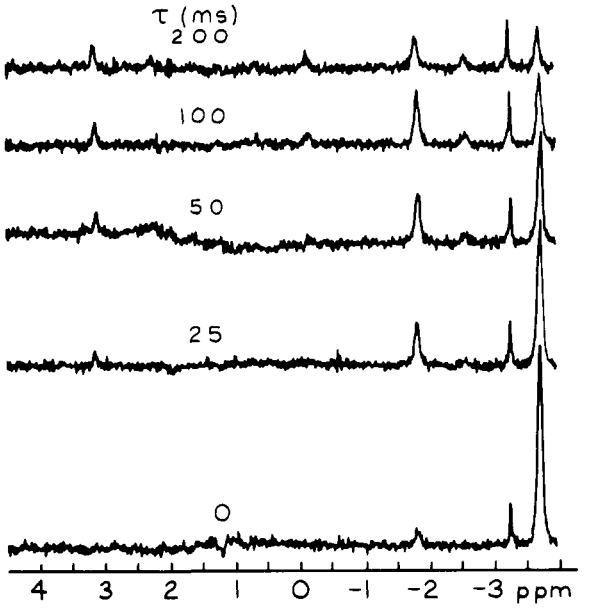

Figure 3. Transient NOE difference spectra resulting from inversion of the Met 80 γ' proton resonance. See Figure 2 for experimental details.

of local structures in proteins, were described.[3-8] Theoretical considerations[3,5] indicate a more favorable situation for NOE studies of macromolecules at high fields than for the more conventional experiments with small molecules under the conditions of extreme motional narrowing. This is because the limiting magnitude of the NOE in macromolecules is larger by a factor 2, and the NOE's are almost completely determined by intramolecular dipole-dipole interactions. On the other hand it was also pointed out that spin diffusion will be of considerable importance in proteins, causing the NOE's to be less specific and hence less useful.[2,9] Here, we describe some experiments with ferrocytochrome *c* to demonstrate that transient NOE experiments[10,11] provide a means for obtaining specific NOE's even in the presence of strong spin diffusion. Ferrocytochrome *c* was particularly suited for this study. Despite the molecular weight of 12 500, the ^{1}H NMR spectrum contains numerous well-resolved lines[12,13] (Figure 1), which could be used to unambiguously outline spin diffusion pathways in this protein.

The high-field portion from 4 to −4 ppm of the 360-MHz ^{1}H NMR spectrum of horse heart ferrocytochrome *c* is shown in the top trace of Figure 1, and different NOE experiments are shown in Figures 1-3. Experimental details are given in the figure captions. We will focus our attention on the high-field shifted resonances of the heme iron ligand Met 80, which are identified in Figure 1 by the greek letters β, β', γ, γ', and ε.[12,13]

The lower traces of Figure 1 show two steady-state NOE difference spectra[7] obtained by irradiation of the Met 80 γ and γ' peaks. NOE's are displayed directly, with negative Overhauser enhancements appearing as positive peaks. The steady-state NOE difference spectra contain a large number of lines which, except for the Met 80 resonances, have not yet been individually assigned. Except for the γ and γ' peaks, the two NOE difference spectra are essentially identical, even though, as will be shown later by the transient NOE studies, the Met 80 γ and γ' protons have substantially different local environments. This is a consequence of cross relaxation.

Transient NOE's observed at variable delay times τ after irradiation of the Met 80 γ and γ' resonances with a selective inversion pulse are shown in Figures 2 and 3, respectively. For increasing τ, the intensity of the pulsed line decreases, while the intensities of the other lines build up by spin diffusion at characteristic rates. After reaching a maximum, the lines decay

to zero via spin-lattice relaxation. The initial buildup rates of the NOE's depend only on the cross relaxation coefficients between the irradiated spin and the observed nuclei, and are thus directly related to the inverse of the sixth power of the proton-proton distances in the three-dimensional structure of the protein.

The following are some details to be observed in the transient NOE's of Figures 2 and 3. At $\tau = 0$, the line corresponding to the geminal methylene proton with respect to the pulsed nucleus has already emerged because of spin diffusion during the 15 ms of the pulse duration. In Figure 3 the additional appearance of the methyl signal ϵ in the $\tau = 0$ trace is a trivial consequence of the limited selectivity of the inversion pulse applied to the line γ'. In both Figures 2 and 3 a line at 3.1 ppm grows at about the same rate as the β-methylene signals of Met 80. From two decoupled NOE difference spectra, where, respectively, the β or β' line was irradiated for spin pumping prior to spin decoupling during data acquisition,[7,8] this resonance was independently assigned to the α proton of Met 80. It is seen that the α-proton resonance grows faster when the γ' peak is pulsed than when the γ peak is pulsed. In Figure 3 the α-proton resonance has already appeared at $\tau = 25$ ms, whereas it has not emerged until 50 ms in Figure 2.

Corresponding transient NOE's were obtained after application of selective inversion pulses to the resonances β and β' (Figure 1). It was found that the α-proton line of Met 80 grows faster after irradiation of resonance β' than after irradiation of β. In an additional experiment the resonances γ and γ' were found to grow faster than β and β' after pulse inversion of the Met 80 methyl line ϵ.

From these experiments the increased information content of transient NOE studies in macromolecules (Figures 2 and 3) as compared to the more conventional steady-state experiments (Figure 1) is readily apparent. While the steady-state NOE was able to distinguish between the β- and γ-methylene protons, the transient NOE's further distinguished between β and β' and γ and γ', respectively, of the axial Met 80. These assignments agree with those generally accepted,[14] which were originally suggested from ring-current calculations based on the X-ray structure.[13] The transient NOE's provided further information on static and dynamic aspects of the spatial arrangement of Met 80 in the protein. The different growth rates of the α-proton line (Figures 2 and 3) clearly show that the protons β' and γ' are located more closely to the α proton than the protons β and γ. Since they are at higher field (Figure 1), the β' and γ' protons must also be closest to the heme ring plane. That the different local environments of the individual β- and γ-methylene protons are manifested in the transient NOE's further shows that the rotational mobility about the single bonds in the side chain of Met 80 is severely limited in ferrocytochrome *c*. Finally, experiments of the type of Figures 2 and 3 provide a convincing demonstration of spin diffusion pathways in proteins. Overall, the present experiments imply that spin diffusion in macromolecules, rather than leading necessarily to less specific and hence less useful NOE's,[2,9] may through suitable use of the two-dimensional frequency-time space of transient NOE experiments lead to novel insights into the molecular structures which might not be available otherwise.

Acknowledgments. Financial support by the Roche Research Foundation for Scientific Exchange and Biomedical Collaboration with Switzerland (fellowship to S. L. Gordon) and the Swiss National Science Foundation (project 3.0046.76) is gratefully acknowledged.

References and Notes

(1) Noggle, J. H.; Schirmer, R. E. "The Nuclear Overhauser Effect", Academic Press: New York, 1971.
(2) Kalk, A.; Berendsen, H. J. C. *J. Magn. Reson.* **1976**, *24*, 343–366.
(3) Balaram, P.; Bothner-By, A. A.; Dadok, J. *J. Am. Chem. Soc.* **1972**, *94*, 4015–4017.
(4) Campbell, I. D.; Dobson, C. M.; Williams, R. J. P. *J. Chem. Soc., Chem. Commun.* **1974**, 888–889.
(5) Glickson, J. D.; Gordon, S. L.; Pittner, T. P.; Agresti, D. G.; Walter, R. *Biochemistry.* **1976**, *15*, 5721–5729.
(6) Keller, R. M.; Wüthrich, K. *Biochim. Biophys. Acta.* **1978**, *533*, 195–208.
(7) Richarz, R.; Wüthrich, K. *J. Magn. Reson.* **1978**, *30*, 147–150.
(8) Wüthrich, K.; Wagner, G.; Richarz, R.; Perkins, S. J. *Biochemistry.* **1978**, *17*, 2253–2263.
(9) Hull, W. E.; Sykes, B. D. *J. Chem. Phys.* **1975**, 867–880.
(10) Solomon, I. *Phys. Rev.* **1955**, *99*, 559–565.
(11) Experiments of the type discussed in this communication were alluded to in the closing paragraph of ref 2. Transient NOE experiments on small molecules have been carried out frequently, for example, Freeman, R.; Hill, H. D. W.; Tomlinson, B. L. *J. Chem. Phys.* **1974**, *61*, 4466–4473.
(12) Wüthrich, K. *Proc. Natl. Acad. Sci. U.S.A.* **1989**, *63*, 1071–1078.
(13) McDonald, C. C.; Phillips, W. D. *Biochemistry.* **1973**, *12*, 3170–3186.
(14) Cookson, D. J.; Moore, G. R.; Pitt, R. C.; Williams, R. J. P.; Campbell, I. D.; Ambler, R. P.; Bruschi, M.; Le Gall, J. *Eur. J. Biochem.* **1978**, *83*, 261–275.
(15) Sodium 2,2,3,3-tetradeuterio-3-trimethylsilylpropionate.
(16) Free induction decays.
(17) School of Chemistry, Georgia Institute of Technology, Atlanta, Georgia 30332.

Sidney L. Gordon,*[17] Kurt Wüthrich*
Institut für Molekularbiologie und Biophysik
Eidgenössische Technische Hochschule
CH-8093 Zürich-Hönggerberg, Switzerland
Received May 17, 1978

Analogues of Metallic Lattices in Rhodium Carbonyl Cluster Chemistry. Synthesis and X-ray Structure of the $[Rh_{15}(\mu\text{-}CO)_{14}(CO)_{13}]^{3-}$ and $[Rh_{14}(\mu\text{-}CO)_{16}(CO)_9]^{4-}$ Anions Showing a Stepwise Hexagonal Close-Packed/Body-Centered Cubic Interconversion

Sir:

We have already reported the isolation and characterization of two members of a family of rhodium carbonyl cluster anions, $[Rh_{13}(CO)_{24}H_{5-n}]^{n-}$ (n = 2, 3), containing a metal atom polyhedron which is part of a hexagonal close-packed lattice.[1] These have been studied by X-ray diffraction[1,2] and by NMR spectroscopy.[3] We report here the characterization of two new high nuclearity rhodium clusters which show different types of metal atom packings. The structural relationships between these two new clusters and the above Rh_{13} species are also discussed.

The mild pyrolysis of $Na_2[Rh_{12}(CO)_{30}]$ or of mixtures of $Rh_4(CO)_{12}$ and NaOH (2.5–3 OH^- for every 15 Rh atoms) in 2-propanol under nitrogen at 80 °C for 10–20 h gives a mixture of brown anionic species. Separation is achieved by fractional precipitation of the alkali metal salts from aqueous solution: after precipitation of sodium salts, potassium salts can be obtained from which $K_3(diglyme)_x[Rh_{15}(CO)_{27}]$ can be separated (15–20% yield) because of its insolubility in diglyme. Metathesis with Me_4N^+ and Et_4N^+ chlorides in methanol gives the corresponding crystalline salts; the ^1H NMR spectrum of the Et_4N^+ salt shows the absence of metal hydrides.

The Me_4N^+ salt has been investigated by X-ray diffraction[4] and the metallic skeleton of the $[Rh_{15}(CO)_{27}]^{3-}$ anion is illustrated schematically in Figure 1a, while Figure 1b shows the metallic coordination around the central metal atom. The metal atom cluster may formally be derived from the polyhedron of D_{3h} symmetry, which contains that part of the hexagonal close-packed array found in the $[Rh_{13}(CO)_{24}H_{5-n}]^{n-}$ (n = 2, 3) cluster (Figure 2), by capping two square faces ((2, 3, 6, 7) and (9, 11, 13, 14) in Figure 1a). However, while the bottom part of the polyhedron follows this hexagonal close

0002-7863/78/1500-7096$01.00/0